

# Generation of maximal snake polyominoes using a deep neural network

Benjamin Gauthier

Alain Goupil

Fadel Toure

Université du Québec à Trois-Rivières, Trois-Rivières, Canada

Benjamin.Gauthier@uqtr.ca

Alain.Goupil@uqtr.ca

Fadel.Toure@uqtr.ca

Maximal snake polyominoes are difficult to study numerically in large rectangles, as computing them requires the complete enumeration of all snakes for a specific grid size, which corresponds to a brute force algorithm. This technique is thus challenging to use in larger rectangles, which hinders the study of maximal snakes. Furthermore, most enumerable snakes lie in small rectangles, making it difficult to study large-scale patterns. In this paper, we investigate the contribution of a deep neural network to the generation of maximal snake polyominoes from a data-driven training, where the maximality and adjacency constraints are not encoded explicitly, but learned. To this extent, we experiment with a denoising diffusion model, which we call Structured Pixel Space Diffusion (SPS Diffusion). We find that SPS Diffusion generalizes from small grids to larger ones, generating valid snakes up to  $28 \times 28$  squares and producing maximal snake candidates on squares close to the current computational limit. The model is, however, prone to errors such as branching, cycles, or multiple components. Overall, the diffusion model is promising and shows that complex combinatorial objects can be understood by deep neural networks, which is useful in their investigation.

## 1 Introduction

In the past 40 years polyominoes and polycubes have been the object of intense investigations from different points of view: combinatorial, algorithmic and statistical physics ([7] and ref. therein, [13]). The problem of finding the length of maximal snake polyominoes in an arbitrary rectangle is still open. The most effective algorithmic approach currently available consists in enumerating all snake polyominoes and then selecting the maximal ones.

Early foundational work on such brute force algorithms was conducted by Jensen [11], who used transfer-matrix methods and enumeration techniques to count polyominoes and tree-like polyominoes. Later work with Guttmann [10] analyzed the asymptotic behavior of polyomino counts using tools from statistical mechanics, showing that the number of polyominoes grows by a factor of about 4.06 when the number of cells increases by one. Since there exists families of snake polyominoes that are in bijection with Fibonacci numbers ([6]), the number of snakes polyominoes grows exponentially with respect to their size and since there is an injection from the set of snake polyominoes of length  $n$  into the set of self-avoiding walks ([6]) the growth constant of snake polyominoes is at most that of self-avoiding walks which is known to be 2.6 ([9]). There is thus an inherent difficulty in generating snakes by exhaustive enumeration, especially in large rectangles.

Barequet and Ben-Shachar [2] revisited polyomino enumeration by introducing bounding boxes rotated by  $45^\circ$  instead of axis-aligned rectangles. This reformulation improved brute-force enumeration and allowed polyominoes up to size 70 to be enumerated, compared to Jensen's previous limit of 56. Nevertheless, the enumeration remains exponential, highlighting the difficulty of counting and generating maximal snakes in large grids.

Another issue is that we observed (without proof) that the general structure of maximal snake polyominoes is different and more apparent in large rectangles compared to small rectangles. Maximal snakes in large rectangles are, so far, impossible to obtain with conventional programming. It becomes relevant to observe maximal snake polyominoes in large rectangles in the hope of formulating conjectures of exact expressions about their size and their enumeration.

A theoretical upper bound on the maximal length of snake polyominoes is provided by the  $2/3$  theorem [14]. While these upper bounds provide useful theoretical guidance, they do not help overcome the computational difficulties of generating maximal snake polyominoes in large rectangles.

Knowing these previous algorithmic limitations, the use of deep neural network (DNN) becomes an interesting alternative to circumvent exponential complexity and study snakes in larger rectangles. Indeed, DNNs have polynomial complexity, which makes them theoretically faster than the current brute force algorithms used for generating snake polyominoes of maximal length. While DNNs have achieved remarkable success in domains such as image generation and natural language processing [20, 8], their application in discrete combinatorial objects and mathematical structure discovery remains relatively unseen to us.

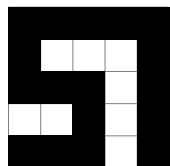
In this work, we generate snake polyominoes using a Structured Pixel Space Diffusion (SPS Diffusion) model. Our goal is not to replace exact methods for enumerating snake polyominoes, but rather to evaluate whether deep neural networks can learn the structural constraints of snake polyominoes and produce candidates for maximal snakes, thus offering an additional tool to classical enumeration techniques and, as a byproduct, an argument for the existence of combinatorial structure of these objects. Section 2 introduces the necessary concepts. In section 3 we introduce two neural networks and compare them. In section 4, we present the results obtained.

## 2 Preliminaries

### 2.1 snake polyominoes definitions

In this section, we recall useful definitions to understand some technical aspects of this research. For a rigorous definition of snake polyominoes, see [12].

A snake polyomino, or more briefly a snake, is a polyomino where all cells are of degree two except for two cells of degree one, called the head and tail. In a grid representation, living cells (black) correspond to the snake body and dead cells (white) to empty cells (Fig. 1a). We use a matrix representation where living cells are labeled 1 and dead cells 0 (Fig. 1b). Snakes are contained in discrete rectangles of size  $H \times W$ , and, naturally, the same goes for their matrix representation. From graph theory, it follows that the degree of a cell  $x$  is the number of edge-adjacent living cells. We assume the standard 4-connectivity of square cells, where each cell has at most four neighbors [4].



$$\begin{bmatrix} 1 & 1 & 1 & 1 & 1 \\ 1 & 0 & 0 & 0 & 1 \\ 1 & 1 & 1 & 0 & 1 \\ 0 & 0 & 1 & 0 & 1 \\ 1 & 1 & 1 & 0 & 1 \end{bmatrix}$$

(a) Grid representation of a snake. (b) Matrix representation of a snake.

Figure 1: Different representations of snake polyominoes.

To qualitatively assess generated snakes, we identify recurring snake-like structures, i.e., patterns commonly observed in maximal snakes (Fig. 2). Examples include stairs, which provide a compact folding of cells of degree at most two [3], triangles of six dead cells, and configurations where the head or tail folds compactly. Such structures frequently appear in maximal snakes, although they are not exclusive. For example, head and tail are frequently observed along the borders and corners of the grid.

Conversely, we identify snake malformations, which are structures incompatible with valid snakes (Fig. 2). Examples include branching, cycles (absence of head and tail), open heads/tails and forests of snakes where several disconnected components appear. The presence of such structures generally indicates that the snake is not maximal. Note that an open head/tail doesn't imply that the snake is not maximal, rather that it may not be. It is also useful to know that density is in general greater along the edges of the grid than in the center. This fact has been proved for  $2D$ -words ([14]). Border density is thus a good indicator that a snake is maximal.

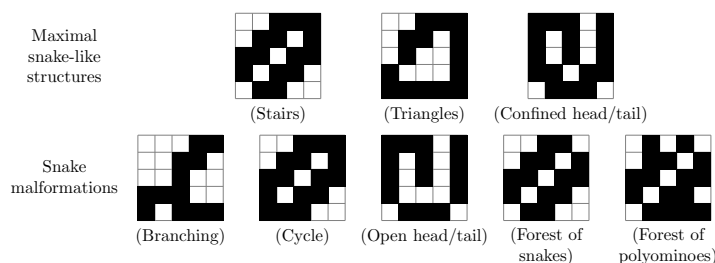


Figure 2: Maximal snake-like structures (above) - stairs, a triangle of dead cells and the confined tail/head. Snake malformations (below) - branching, cycle, forest of snakes and an open head/tail. Note that for the open head/tail, the disjointed segments should be considered part of the same snake, as if the grid was bigger than shown here.

## 2.2 Deep neural network definitions

In the SPS diffusion model to be introduced later, data are represented as matrices. The source (**src**) is the input of the model, the target (**tgt**) the expected output, and the output (**out**) the model prediction. The model itself is a parameterized function represented by a deep neural network and learned from data.

Training consists in minimizing a loss function that measures the discrepancy between **out** and **tgt**. The parameters of the neural network are updated using gradient descent combined with backpropagation, which computes the gradient of the loss with respect to the model parameters [18].

A fundamental layer of diffusion model is the convolutional layer, which is itself a neural network component that applies small learnable filters (kernels) across an input (such as an image) to extract local patterns. Each filter slides over the input and computes dot products, producing feature maps that detect structures such as edges, textures, or shapes. Convolutional layers are central to diffusion models and enable the efficient capture of spatially localized features, which is particularly important for modeling snakes. [17]

Finally, we define self-attention, which is a neural network mechanism that allows a model to contextualize different parts of an input to one another. Given a set of input representations, the layer computes queries, keys, and values, and determines how strongly each element should attend to the others through similarity scores (attention scores). This produces weighted combinations of the values, enabling the model to capture long-range dependencies and global structure. In spatial settings such as snake polyomino generation, positional information is incorporated using 2D Rotary Positional Em-

beddings (RoPE-2D) [19], which encode relative spatial relationships while preserving the ability of attention to model interactions across the grid. [20]

### 3 Methodology for the SPS Diffusion model

#### 3.1 Snake generation

We investigate the use of a denoising diffusion probabilistic model (DDPM) for generating maximal snakes. Our variant of this type of model is referred to as structured pixel space diffusion (SPS Diffusion), for reasons that will be detailed in Sec. 3.2.

The process of generating polyominoes with SPS Diffusion is directly analogous to image generation with a standard DDPM and it is described as follows:

1. An image of pure noise, sampled from a normal distribution, is initialized and given to the model.
2. At each step, the model predicts the amount of noise to be removed from the sample in order to move closer to a structured configuration.
3. The predicted noise is subtracted from the current sample.
4. The updated sample is fed back into the model, and the process is repeated for a given number of steps. A larger number of steps typically yields higher-quality outputs.

Fig. 3 illustrates the evolution of an image from pure noise to a maximal snake. This process is called *backward diffusion*. As in standard DDPMs, the backward diffusion process is described by Eq. (1).

$$\mathbf{x}_{t-1} = \frac{1}{\sqrt{\alpha_t}} \left( \mathbf{x}_t - \frac{\beta_t}{\sqrt{1-\alpha_t}} \varepsilon_\theta(\mathbf{x}_t, t) \right) + \sqrt{\frac{1-\alpha_{t-1}}{1-\alpha_t}} \beta_t \varepsilon \quad (1)$$

where  $\mathbf{x}_t$  is the image at step  $t$ ,  $\varepsilon_\theta(\mathbf{x}_t, t)$  is the prediction of the model and  $\varepsilon \sim \mathcal{N}(0, 1)$  is a statistical variable following a normal distribution of average 0 and variance 1. [5] The image  $\mathbf{x}_0$  is the fully denoised image (a maximal snake ideally), and the image  $\mathbf{x}_T$  is the pure noise image (noisy polyomino). The other symbols are constants that are related to the Normal distribution that governs the forward diffusion process, detailed later in Sec. 3.3. See [5] for the complete definitions.

#### 3.2 Differences between SPS Diffusion and Stable Diffusion

SPS Diffusion operates similarly to Stable Diffusion: a noisy image is iteratively denoised until the final output emerges. However, maximal snakes are structurally much simpler than natural images. Polyominoes are represented in binary form, with a single feature channel taking values 0 (white) or 1

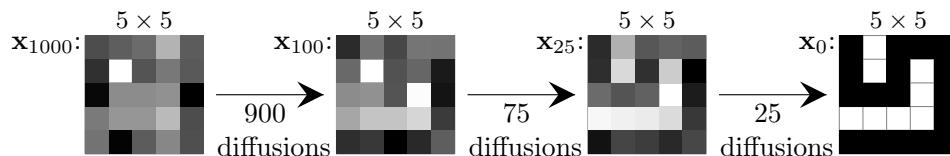


Figure 3: The backward diffusion process to obtain a maximal snake using an SPS Diffusion model. The arrows indicate the number of diffusion steps used for the next image ( $\mathbf{x}_t$ ). The initial pure noise image  $\mathbf{x}_{1000}$  is diffused into a maximal snake image  $\mathbf{x}_0$ .

(black). In practice, this channel initially takes values in  $\mathbb{R}$  and is rounded to the nearest integer only at the end, which explains the gray cells visible during the backward diffusion process in Fig. 3.

In contrast, natural images typically use three feature channels (red, green, blue), each ranging from 0 to 255, yielding over 16 million possible colors. Moreover, unlike Stable Diffusion, the model is not conditioned on text or image prompts: the generation always converges to a specific family of images, namely maximal snakes. Finally, snake grids contain far fewer pixels than photographic images; in practice they are smaller than  $64 \times 64$ , whereas natural images often exceed  $512 \times 512$  pixels. These differences necessitate modifications to the standard Stable Diffusion architecture.

**First**, our model does not include a Contrastive Language–Image Pretraining (CLIP) encoder. In Stable Diffusion, CLIP is used to project text and image data into a shared embedding space, enabling training on text–image pairs. CLIP can also serve as a loss function to measure how well a generated image matches a textual prompt [15]. Since maximal snake polyomino generation involves no prompts, this module is unnecessary.

**Second**, the model does not require a Variational Autoencoder (VAE). In Stable Diffusion (or more generally, Latent Diffusion models), the VAE compresses images from pixel space into a latent space to reduce computational cost, since the U-Net cannot practically process very large images directly [16]. Snake images, however, are already very small, making such a compression step useless.

**Third**, the model is composed solely of a U-Net. As in Stable Diffusion, the U-Net predicts the noise to be removed from the current sample. To achieve this, the U-Net reduces the spatial resolution of the input as it applies successive convolutional layers, a process known as downsampling [17]. However, because snake polyomino images are already small, excessive downsampling would collapse the structural information in the image entirely. While a typical Stable Diffusion U-Net may employ 5 or 6 levels of downsampling, SPS Diffusion is restricted to only 3 levels to preserve structural fidelity. For these reasons, this U-Net is better referred to as a mini U-Net. Each level of the mini U-Net applies several convolutions to the image, followed by a self-attention computation which uses RoPE 2D.

Since there is no VAE, there is no latent space, thus only leaving the pixel space in which the polyomino images live. Also, because this model is specialized in denoising 2D structures, we call it Structured Pixel Space Diffusion (SPS Diffusion). This model is architecturally simpler than Stable Diffusion, having only a single mini U-Net.

Fig. 4 presents the SPS Diffusion model architecture. The model is built from residual blocks, which let information pass through while refining features, and attention blocks, which help to focus on the most important parts of the input. The network has multiple levels which process the image at different resolutions: lower levels handle fine details, higher levels capture larger patterns. The bottleneck is the middle stage where the image is the smallest and most abstract, compressing information before reconstruction. Downsampling is done using a specific way of doing convolution, where the kernel is slid across the image 2 pixels at a time, instead of 1 pixel at a time. Upsampling is done using nearest-neighbor interpolation, which enlarges the image back toward its original size. Skip connections link matching levels in the encoder and decoder, adding the feature channels from the encoder to the decoder to help recover fine details more accurately.

### 3.3 Training

Sec 3.1 explains how polyomino images are generated using the SPS Diffusion model. This process is called backward diffusion, because noise is removed from the image instead of being added. When training DDPM models, we use *forward diffusion*, where noise is added to a known solution  $\mathbf{x}_0$ , a maximal snake, in order to generate the **src** data for training. In other words, the noisy polyominoes  $\mathbf{x}_t$  (**src**), are

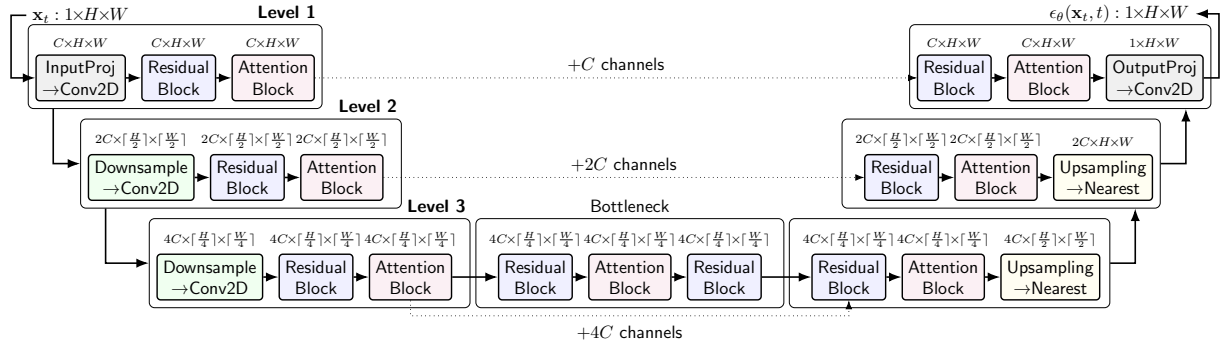


Figure 4: Architecture of the SPS Diffusion model. The model is given  $\mathbf{x}_t$ , which returns the noise to remove  $\epsilon_\theta(\mathbf{x}_t, t)$  (Sec. 3.3 discusses this further). The labels for the image size indicate the dimensions after the operation of the block below has been applied.

computed in training. Eq. (2) shows how  $\mathbf{x}_t$  is computed. The constant  $\bar{\alpha}_t$  is related to the mean and variance parameters of the normal distribution governing the forward diffusion process. See [5] for the full definition.

$$\mathbf{x}_t = \sqrt{\bar{\alpha}_t} \mathbf{x}_0 + \sqrt{1 - \bar{\alpha}_t} \epsilon \quad (2)$$

Since the model estimates the noise term  $\epsilon_\theta(\mathbf{x}_t, t)$  (see Eq. (1)) that should be removed from  $\mathbf{x}_t$  to recover a sample closer to  $\mathbf{x}_0$ , the training target **tgt** corresponds to the actual noise  $\epsilon$  that was added during the forward diffusion step linking  $\mathbf{x}_{t-1}$  and  $\mathbf{x}_t$  (Eq. (2)). Thus, the training pair (**src**, **tgt**) consists of **src** =  $\mathbf{x}_t$ , the noisy polyomino at timestep  $t$ , and **tgt** =  $\epsilon$ , the true noise added at that step.

The SPS Diffusion model presented here was trained by computing the **src** (a noisy polyomino) using known maximal snakes for rectangles of dimension  $W \leq 50$  and  $H \leq 14$ . The noise  $\epsilon$  that was added to the maximal snakes during the computation is the **tgt**, as per Eq. (2).

For the loss function, we use the Mean Squared Error (MSE), as it is the one that performs best. We experimented with several loss functions, but none came close to the performance of MSE, which is good at generating snake-like structures for any grid size, unlike all the other loss functions tested which often produced snake malformations (Sec. 2). MSE is defined as follows:

$$\text{MSE}(\mathbf{out}, \mathbf{tgt}) = \frac{1}{N} \sum_{ij} (\mathbf{tgt}_{ij} - \mathbf{out}_{ij})^2 \quad (3)$$

## 4 Results for the SPS Diffusion model

We look at the performance of SPS Diffusion under different grid sizes. We consider a SPS Diffusion model trained on over 200 different grid sizes, ranging from small grids of size  $4 \times 4$  to large rectangular grids of  $50 \times 10$ . We start with grids for which the grid sizes have been seen by the model during training, as shown in Fig. 5. SPS Diffusion has little difficulty generating maximal snake polyominoes in all grid sizes seen during training.

Looking at grids not seen by the model during training in Fig. 6, SPS Diffusion is able to generalize its understanding of snake polyominoes in small grids to much larger grid sizes at inference time, that is, generate snake-like structures even in large grids where the positional encoding is technically different.

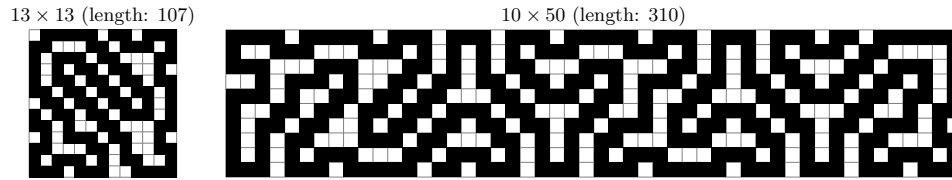


Figure 5: Two maximal snakes generated by the SPS Diffusion model in grids seen during training.

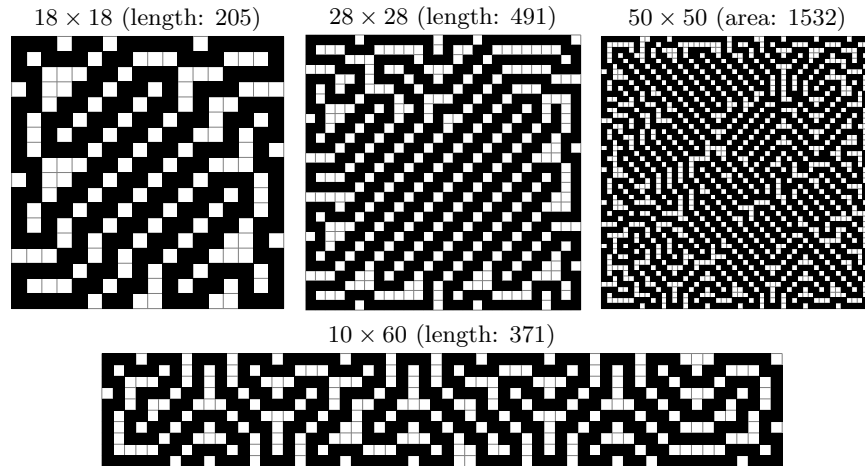


Figure 6: Results generated by the SPS Diffusion model in grids not seen during training.

Furthermore, we were able to generate snake polyominoes for square grid sizes up to  $28 \times 28$ , which is bigger than the maximum size used in training for squares ( $14 \times 14$ ). Similarly, for many rectangular grids, ranging from nearly square grids to very elongated rectangles of size  $10 \times 60$ , we were also able to generate several snakes. When trying to generate snakes in very large grid sizes, we hit the limitations of the model. Fig. 6 shows a polyomino that was generated at a larger grid size, more specifically of size  $50 \times 50$ . Although we observe snake-like structures in the grid, the structure itself is not a snake. In some cases, we obtain a forest of snakes, in others, we obtain forests of polyominoes, which are not snakes. Considering the complexity of maximal snakes, the fact that SPS Diffusion is able to get close to a valid solution is encouraging.

Moreover, we were able to generate maximal snakes for grid sizes up to  $17 \times 17$ , which is the current computational limit for squares ([1]). After this bound, we cannot know for certain if the generated snakes are maximal. However, we can estimate a lower bound on the minimal length of maximal snakes and, for several grid sizes, we can sometimes exceed the lower bound by up to 3 cells. We observe that as the grid size increases, it becomes harder for the model to generate a snake, and even harder for a maximal snake. In other words, the error rate increases with the grid size. We also observe that the model makes fewer errors on rectangular grids, where snakes are easier to generate.

The aforementioned limit of  $28 \times 28$  for squares containing a snake is a consequence of this fact. For example, for more than 25 000 images generated, no snakes were produced for a  $29 \times 29$  grid, only forests of snakes and forests of polyominoes. We expect that with more calculation time, snakes could be generated for larger grid sizes, but then we would encounter the initial limitations of the brute force algorithm, that is, calculation time.

While the SPS Diffusion model generates valid snakes in large grids, it has also produced snakes

whose lengths exceed the best previously reported lower bounds. These bounds are rigorous rather than conjectural, as snakes of these lengths have been explicitly constructed, often by hand.

Before these results were obtained, the SPS Diffusion model was trained on a smaller dataset of grids smaller than  $20 \times 10$ . In this setting, the model generated snakes in square grids up to  $23 \times 23$ . After adding square grids up to  $14 \times 14$  (and additional rectangular grids) to the training data, the model generated snakes up to  $28 \times 28$ . This improvement suggests that the model benefits substantially from additional data. Consequently, one possible approach is to generate new snakes with the model itself and include them in the training set for retraining. Such an iterative procedure could improve predictions in larger grids, although it cannot guarantee that the produced snakes are maximal and mainly serves to guide theoretical investigation of maximal snake lengths.

This procedure can in principle be repeated to generate increasingly large snakes, although it currently requires significant computational time. The SPS Diffusion model also makes several errors and produces forbidden patterns such as cells of degree 3 (branching), cycles, forests of snakes and polyominoes, requiring more computation time in order to generate valid snakes, which, even then, yields only a few snakes, and even less maximal snakes.

Moreover, in larger grids there is no guarantee that the positional encoding used for smaller grids (RoPE 2D in the attention layers) will remain effective. The current mini-U-Net architecture is also fixed, with only three downsampling layers, which may be insufficient to capture global positional context in larger grids. This limitation could be mitigated by training a larger U-Net while excluding smaller grids from the training data. Overall, further optimization of the model implementation and evaluation on larger grids will be necessary for long-term applicability.

## 5 Conclusion

In this work, we explored the use of a deep neural network to generate maximal snake polyominoes from data, with the goal of overcoming the exponential complexity of traditional brute force algorithms, as well as studying maximal snakes in larger grid that are impossible to compute by enumeration. In this case, we used a diffusion model which we call Structured Pixel Space Diffusion (SPS Diffusion).

Our experiments show that SPS Diffusion generates good results, as it can easily reproduce the data it was trained with, as well as generalizing to larger rectangles. More specifically, for square grids, snakes were generated up to  $28 \times 28$ , and their length was close to the previously known lower bound. For some configurations, the previously known bound was exceeded by one cell, which demonstrates the potential of the approach when given more training and refinements. The main weakness of SPS Diffusion is that it generates snake malformations, including branching, cycles, and forests. Also the likelihood of generating a valid snake decreases as the grid size increases. These results support the idea that diffusion models can capture nontrivial combinatorial structures directly from examples, even when the constraints are not explicitly programmed into the model.

Several directions remain open. On the modeling side, reducing invalid generations and improving scalability to larger grids are key objectives, for instance by modifying the architecture and the positional encoding of the cells. Alternatively, the loss function could also be tweaked to speed up and improve the training.

On the combinatorial side, a more systematic analysis of recurring substructures in the generated candidates could help guide future conjectures about maximal snake size in large rectangles. Overall, deep neural network models, and SPS Diffusion in particular, provide a new numerical tool to explore maximal snakes beyond the range of exhaustive enumeration.

## References

- [1] [A331968 - OEIS](https://oeis.org/A331968). Available at <https://oeis.org/A331968>.
- [2] Gill Barequet & Gil Ben-Shachar (2024): Counting Polyominoes, Revisited. In: *2024 Proceedings of the Symposium on Algorithm Engineering and Experiments, ALENEX 2024*, Proceedings of the Workshop on Algorithm Engineering and Experiments, pp. 133–143. Publisher Copyright: Copyright © 2024 by SIAM.; 2024 SIAM Symposium on Algorithm Engineering and Experiments, ALENEX 2024 ; Conference date: 07-01-2024 Through 08-01-2024.
- [3] Alexandre Blondin Massé, Alain Goupil, Raphael L’Heureux & Louis Marin (2025): Maximal 2-Dimensional Binary Words of Bounded Degree. In: *International Conference on Combinatorics on Words*, Springer, pp. 37–48.
- [4] Reinhard Diestel: Graph Theory. *Graduate Texts in Mathematics* 173, Springer, doi:10.1007/978-3-662-70107-2. Available at <https://link.springer.com/10.1007/978-3-662-70107-2>.
- [5] Benyamin Ghogh & Ali Ghodsi (2024): Diffusion Models: Tutorial and Survey, doi:10.31219/osf.io/w7jcm.
- [6] Alain Goupil, Marie-Eve Pellerin & Jérôme de Wouters d’oplinter (2018): Partially directed snake polyominoes. *Discrete Applied Mathematics* 236, pp. 223–234.
- [7] Anthony J Guttmann (2009): History and introduction to polygon models and polyominoes. In: *Polygons, Polyominoes and Polycubes*, Springer, pp. 1–21.
- [8] Jonathan Ho, Ajay Jain & Pieter Abbeel (2020): Denoising Diffusion Probabilistic Models. arXiv:2006.11239.
- [9] Jesper Lykke Jacobsen, Christian R Scullard & Anthony J Guttmann (2016): On the growth constant for square-lattice self-avoiding walks. *Journal of Physics A: Mathematical and Theoretical* 49(49), p. 494004.
- [10] Iwan Jensen (2001): Enumerations of Lattice Animals and Trees. *Journal of Statistical Physics* 102(3–4), p. 865–881, doi:10.1023/a:1004855020556. Available at <http://dx.doi.org/10.1023/A:1004855020556>.
- [11] Iwan Jensen & Anthony J Guttmann (2000): Statistics of lattice animals (polyominoes) and polygons. *Journal of Physics A: Mathematical and General* 33(29), p. L257–L263, doi:10.1088/0305-4470/33/29/102. Available at <http://dx.doi.org/10.1088/0305-4470/33/29/102>.
- [12] Raphaël L’Heureux: Recherche des serpents et des forêts de serpents maximaux dans le plan approches exhaustives et apprentissage machine. Available at <https://depot-e.uqtr.ca/id/eprint/10534/>.
- [13] Alexandre Blondin Massé, Julien De Carufel & Alain Goupil (2018): Saturated fully leafed tree-like polyforms and polycubes. *Journal of Discrete Algorithms* 52, pp. 38–54.
- [14] Alexandre Blondin Massé, Alain Goupil, Raphael L’Heureux & Louis Marin: Maximal 2-dimensional binary words of bounded degree, doi:10.48550/arXiv.2505.13640. arXiv:2505.13640 [math].
- [15] Alec Radford, Jong Wook Kim, Chris Hallacy, Aditya Ramesh, Gabriel Goh, Sandhini Agarwal, Girish Sastry, Amanda Askell, Pamela Mishkin, Jack Clark, Gretchen Krueger & Ilya Sutskever: Learning Transferable Visual Models From Natural Language Supervision, doi:10.48550/arXiv.2103.00020. arXiv:2103.00020 [cs].
- [16] Robin Rombach, Andreas Blattmann, Dominik Lorenz, Patrick Esser & Bjorn Ommer: High-Resolution Image Synthesis with Latent Diffusion Models. In: *2022 IEEE/CVF Conference on Computer Vision and Pattern Recognition (CVPR)*, IEEE, pp. 10674–10685, doi:10.1109/CVPR52688.2022.01042. Available at <https://ieeexplore.ieee.org/document/9878449/>.

- [17] Olaf Ronneberger, Philipp Fischer & Thomas Brox: U-Net: Convolutional Networks for Biomedical Image Segmentation, doi:10.48550/arXiv.1505.04597. arXiv:1505.04597 [cs].
- [18] Sebastian Ruder: An overview of gradient descent optimization algorithms, doi:10.48550/arXiv.1609.04747. arXiv:1609.04747 [cs].
- [19] Jianlin Su, Yu Lu, Shengfeng Pan, Ahmed Murtadha, Bo Wen & Yunfeng Liu: RoFormer: Enhanced Transformer with Rotary Position Embedding, doi:10.48550/arXiv.2104.09864. arXiv:2104.09864 [cs].
- [20] Ashish Vaswani, Noam Shazeer, Niki Parmar, Jakob Uszkoreit, Llion Jones, Aidan N. Gomez, Lukasz Kaiser & Illia Polosukhin: Attention Is All You Need, doi:10.48550/arXiv.1706.03762. arXiv:1706.03762 [cs].